

GRAVITY DEFORMATION MEASUREMENTS OF 70m REFLECTOR SURFACES

Michael Brenner

Engineering Metrology Services

Tucson, AZ 85704

Michael J. Britcliffe and William A. Imbriale

California Institute of Technology, Jet Propulsion Laboratory

Pasadena, CA 91109

Abstract

Two of NASA's Deep Space Network (DSN) 70-meter reflectors are measured using a Leica TDM-5000 theodolite. The main reflector surface was measured at five elevation angles so that a gravity deformation model could be derived that described the main reflector distortions over the entire range of elevation angles. The report describes the measurement equipment and accuracy and the results derived from the data.

Keywords: surface measurements, gravity deformation, 70-meter antennas

1. Introduction

One of NASA's current technology initiatives is to increase deep space communications capacity by the implementation of Ka-Band (32 GHz) reception on all Deep Space Network (DSN) antennas. A major problem for Ka-band on the 70-meter antennas is the loss in gain with elevation angle due to gravity induced structural mechanical distortions of the main reflector surface. One of the proposed solutions is to use a Deformable Flat Plate (DFP) in the optics path to compensate for the main reflector distortions. However, the design of the DFP requires knowing the actual surface shape over all elevation angles. The initial experiment on the 70-meter antenna used holographic measurements at three lower elevation angles to predict the surface over the entire elevation range. Holography does not provide a direct measurement of the surface above 47 degrees and relies on extrapolation of the lower angle data to predict the surface at high elevation angles. Therefore the accuracy of the high elevation surfaces is unknown. Also, the measured efficiencies of DSS-14 and DSS-43 over elevation angle as show in [1] differ significantly. Consequently, Michael Brenner of Engineering Metrology Services (EMS) measured the DSS-14 and DSS-43 main reflector surfaces over the full range of elevation angles using a ranging theodolite. This report describes the meas-

urement equipment and accuracy and the results derived from the data.

2. Equipment and Accuracy

Most of the measurements described in this document were made using a Leica TDM-5000 "total station" theodolite as shown in Figure 1 tied into a portable PC with measurement software. The instrument measures vertical and horizontal angles and distances, downloads them to the PC with MeasTools© [2] software which converts the coordinates from the spherical to a Cartesian system, manages coordinate transformations, and can be used to command the instrument to motor to a desired look angle.

The inherent instrument accuracies are:

- Angle accuracy ± 1 arc second
- Estimated operator angle accuracy ± 3 arc second
- Distance accuracy with tape targets ± 0.050 inch

During the nighttime measurements, the average temperature was close to 40°F. The resulting 27-PPM (0.040 inch at the perimeter of the main reflector) distance measurement bias was compensated in software.

3. Targeting

In this procedure, 20 mm square tape targets 0.013" thick (see Figure 2) were attached to the front face of JPL black plastic targets such that the visible target cross-hair was 0.439 inches above and normal to the local reflector surface. As stated above, the estimated target height variation is on the order of ± 0.015 inch.

4. Measurement Procedure

The theodolite was bolted securely to the bracket close to the center of the main reflector. Its gravity compensator was turned off so that it would rotate with the reflector. Targets were placed in 12 concentric rings wherever cables, supports or other equipment in the feed support struc-

ture.



Figure 1 – Leica TDM-5000 Theodolite



Figure 2 – Single Target

did not block the view. Cables were tied back out of the way as much as possible. Figure 3 shows the 367 visible target positions on DSS-14 for the zenith measurements. A similar set of targets was used for DSS-43. The view in the figure is as the targets might appear facing the reflector surface with the main reflector at horizon. A picture of some of the targets on DSS-14 is shown in Figure 4. At other angles, fewer targets were visible due to movement of feed structure cable bundles as the reflector rotated to a new position.

5. Measurement Error

The total station theodolite measures distance and angle measurements from the instrument to the target on the reflector surface. The measurement geometry is shown in Figure 5. The range and angle data is used to compute the

error normal to the reflector surface for surface adjustment or to half-path-length error for antenna efficiency calculations.

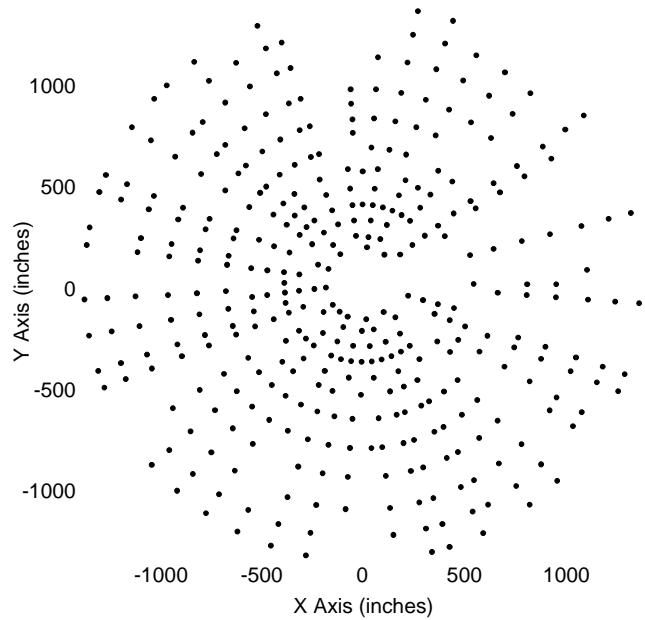


Figure 3 – Visible Target Placement



Figure 4 – Multiple Targets on DSS-14

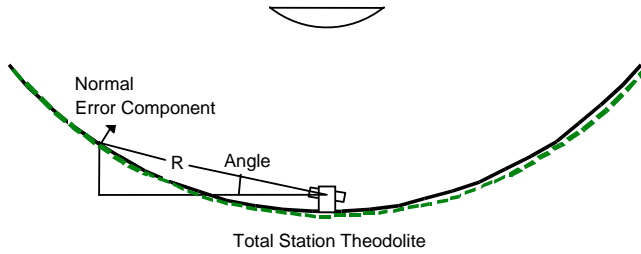


Figure 5 – Reflector Measurement Geometry

The major error contributors are the angle reading error, distance measurement error and targeting error. By viewing a target as closely as possible to tangent to the surface, the effect of distance measurement error inherent in the theodolite is minimized. The farthest target is 36.44 meters (1435 inches) from the vertex of the main reflector. Using this distance with the estimated operator angle accuracy ± 3 arc second gives a peak surface-normal measurement error of ± 0.0209 inch.

For a parabolic main reflector with a theodolite at the vertex, the slope of the theodolite line-of-sight to any target is half of the parabola surface slope at the target. For this shaped main reflector with a nominal focal length of 1065 inches, the edge slope at 35-meter radius is 33° , so the reflector surface is tilted by as much as 16.5° to the theodolite line-of-sight. Based on a distance measurement error of 0.050 inch, this component of the measurement error is $0.050 \tan(16.5^\circ) = \pm 0.0148$ inch. It is estimated that target height variation is on the order of ± 0.015 inch.

Figure 6 shows the estimated 1 sigma measurement error normal to the surface as a function of distance from the instrument to the target. The angle, range and targeting error components are shown with the RSS total and the area weighted 1 sigma RMS half-path-length error of 0.17mm (0.0067 inches).

This error estimate is for the absolute accuracy of the measurement. The error in a surface with accuracy better than 0.17mm RMS could not be resolved. This is also the limit of the accuracy that could be achieved by adjusting a surface with a higher RMS using data from these measurements.

For differential measurements such as studies of the effect of gravity deformation on antenna efficiency where the measured difference is taken for the entire reflector the resolution is much higher. The errors in angle and distance

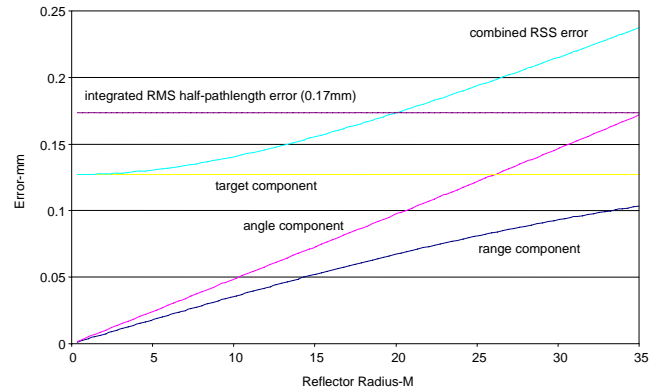


Figure 6 – Measurement Error (1 sigma)

tend to cancel. The targeting error cancels directly. This is verified by the standard deviation of 0.07mm (0.0026 inches) for three measurements of DSS-14 at an elevation angle of 89 degrees. This is the best estimate of the resolution for differential changes of the entire reflector.

6. Coordinate Systems and Data Analysis

The reflector right-handed Cartesian coordinate system is shown in Figure 3. The X-axis is horizontal and parallel to the elevation axis. The Y-axis is vertical positive UP with the main reflector pointed at horizon. The Z-axis is the boresight axis from the vertex to the focus. The reflector coordinate system is based on a reference file created from the nominal target locations. First the nominal target coordinates were calculated based on the measured reflector surface arc length, circumferential spacing and reflector radial surface shape, and combined into a reference file. The theodolite system motored to the nominal location of each target, the target was placed precisely in the theodolite crosshairs, then measured and recorded. When all of the targets were measured the first time at zenith, the data were bestfit to the theoretical coordinates in the reference file to transform the coordinates from a theodolite-centered coordinate system to the reflector system. No reference points, which might indicate the true reflector optics, were used in any of the measurements. The recorded target locations thus transformed became the new reference target file used in all subsequent measurements.

Subsequent to storing the measured coordinates in the reflector coordinate system the data was copied into AnTools© [3] software, which fits the measured data points to the theoretical surface of the shaped main reflector, reports residual surface errors, calculates RMS accuracy and provides surface error plots. Results are presented as Half Path Length Errors (HPL) in thousandths of an inch (mils). The HPL is the usual presentation of surface errors which relates surface RMS with gain loss [4].

Table 1 shows the AnTools© calculation of the RMS errors after best fitting for DSS-14. The best fitting applied performed a least-squares fit using 6 degrees of freedom: translation in x, y and z, rotation about x and y and focal point adjustment since there is a motorized subreflector. The first data row is for all measured points. The second row removes the inner panel, which is blocked by the

subreflector, and the outer panel, which was not included in the holographic measurement or alignment. Since the AnTools© program was not supplied the correct as designed surface for the outer edge points, the RMS using all the points is larger than might be expected.

An error was later discovered in the 30-degree data and the data set subsequently was not used to generate an all angles

	13 deg		30 deg		47 deg		68 deg		89 deg #1		89 deg #2		89 deg #3	
	RMS	Meas	RMS	Meas	RMS	Meas	RMS	Meas	RMS	Meas	RMS	Meas	RMS	Meas
RMS of All Targets (mils)	80	309	74	333	77	348	72	344	79	366	80	367	75	346
RMS with Inner and Outer Targets Removed (mils)	40	259	41	279	34	294	45	292	50	311	48	309	51	298

Table 1 – Measured RMS Errors for DSS-14

model. Two separate nighttime zenith measurements were performed on subsequent nights to determine the measurement repeatability. Additionally the reflector was again measured at zenith, this time during the day, included as #3. The data was best fit to the shaped surface as described above and the residual Half Path Length Errors were compared.

The file shows that based 335 points common to the two nighttime measurements, the RMS of the difference between them is 14.4 mils, which is consistent with a 10-mil RMS measurement accuracy applied to two separate measurements. The RMS difference between measurement #3 (daytime) and the average of the nighttime data is 17.8 mils. Taking the RSS difference to remove measurement error from the thermal effects gives an estimate of 10.4 mils for the RMS of the thermal error. This number is so close to the noise level of the measurements that its significance is questionable. In any case, the results indicate that thermal effects on the main reflector at zenith are small, and probably insignificant.

A similar set of measurements was also carried out at DSS-43 and the data is shown in Table 2. In this case, the correct outer edge design was used in the data analysis.

7. Measurement of Gravity SAG

With minor adjustments to the theodolite and a comfortable working platform for the operator, primary surface and subreflector position measurements as described above can be performed at any elevation angle for a tracking antenna. For antenna structures that behave in a linear elastic fashion, measurements at 3 separate elevation angles provide sufficient information to determine the relative positions of all targets at any other angle. (A common example of non-

linear structural deformation is the bending of bolted flanges.) The process requires the intermediate calculation of the face-up (zenith pointing) and face-side (horizon pointing) gravity deformations of the reflector, and their subsequent vector superposition. The best results will be achieved if the elevation angles at which measurements are made are well separated, such as 0, 45 and 90°. In this case, the analysis was based on 13, 47 and 89°.

The gravity deformation of a linear elastic structure at any elevation angle can be derived by vector superposition of the face-up and face-side gravity vectors as

$$\delta = \delta_u \sin\theta + \delta_s \cos\theta$$

$$\delta_s = \text{face-side gravity deformation}$$

$$\delta_u = \text{face-up gravity deformation}$$

The face-up and face-side deformations described here are of the type derived from a computer structural analysis in which gravity is "turned on" from a particular direction. As such, they cannot be directly measured in the real world. For a linear elastic structure that rotates from angle θ_1 to θ_2 the relative deformation, or motion, will be $\delta_2 - \delta_1$ as shown above. For 3 measurements, two independent linear equations can be written for $\delta_2 - \delta_1$ and $\delta_3 - \delta_1$

$$\begin{bmatrix} \delta_u \\ \delta_s \end{bmatrix} = \begin{bmatrix} \sin\theta_2 - \sin\theta_1 & \cos\theta_2 - \cos\theta_1 \\ \sin\theta_3 - \sin\theta_1 & \cos\theta_3 - \cos\theta_1 \end{bmatrix}^{-1} \begin{bmatrix} \delta_2 - \delta_1 \\ \delta_3 - \delta_1 \end{bmatrix}$$

Now that δ_u and δ_s are known, for any angle θ , the predicted alignment error at a target is the gravity deformation traveling from a measured reference angle (θ_2) to angle θ superposed onto the actual measured alignment error at the reference angle (δ_θ). This can be expressed as

$$\delta(\theta) = \delta_\theta + \delta_u (\sin\theta_2 - \sin\theta) + \delta_s (\cos\theta_2 - \cos\theta)$$

The gravity deformations of the reflector were analyzed in the steps described below:

- After removing the outer and inner rows, the best fit parameters for each set of measured data was determined. The Half Path Length Errors (for ALL the data points) after best fitting were stored in text files.

	13 degrees	30 degrees	47 degrees	68 degrees	89 degrees
RMS of All Targets (mils)	51	49	52	66	64
RMS with Inner and Outer Targets Removed (mils)	38	31	33	41	49

Table 2 – Measured RMS Errors for DSS-43

calculated at 5° elevation intervals from 0 to 90°, plus 13, 30 (for DSS-43 only), 47, 68 and 89° using the actual measured data. By definition, the predictions at 13, 47 and 89° perfectly matched the input data.

- The gravity analysis was performed using the measurement data from 13, 47 and 89° elevation. The predicted HPLE's at each of the common points were calculated at 5° elevation intervals from 0 to 90°, plus 13, 30 (for DSS-43 only), 47, 68 and 89° using the actual measured data. By definition, the predictions at 13, 47 and 89° perfectly matched the input data.
- The above process was repeated, recording the predicted gravity deformations with respect to the nominal rigging angle of 47° elevation.

The RMS data are summarized in Figures 7 and 8 for DSS-14 and DSS-43. The curves show that the measured data at 68 degrees (and 30 degrees for DSS-43) closely match the predicted values. To further emphasize the fact that the gravity predictions from the three angle data match the data at the other measured data, the surface plots of the measured data at 30 and 68 degrees compared to the predicted data using only the 13, 47 and 89 degree data for DSS-43 is shown in Figures 9 and 10. For 30 degrees the predicted RMS was 38.7 mils and the measured RMS was 38.4 mils. For 68 degrees, the results were 47.6 and 47.7 mils respectively.

8. Efficiency Calculations and Measurements

Using the all angle main reflector surface shape data in a Physical Optics calculation with the 70-meter feed and subreflector configuration an efficiency value was determined for both DSS-14 and DSS-43. This predicted efficiency value is compared to the measured efficiency at DSS-14 in Figure 11. This demonstrates that the DSS-43

- A sorting program was written to extract out the measurement points common to all six data files
- The gravity analysis was performed using the measurement data from 13, 47 and 89° elevation. The predicted HPLE's at each of the common points were

main reflector surface gravitational distortion is comparable to DSS-14 and that the measured efficiency difference between DSS-14 and DSS-43 as shown in [1] must be due to other factors, not the main reflector shape.

9. Acknowledgement

The research described in this paper was carried out at the Jet Propulsion Laboratory, California Institute of Technology, under a contract with the National Aeronautics and Space Administration.

10. References

- [1] Sniffin, R. W., "DSMS Telecommunications Link Design Handbook", Jet Propulsion Laboratory internal document D-19379 Rev. E, Jan 15, 2001
- [2] <http://www.engr-metr.com/meastools.html>
- [3] <http://www.engr-metr.com/antools.html>
- [4] Ruze, J., "Antenna Tolerance Theory – A Review", Proc. IEEE, Vol 54, pp 633-640, 1966

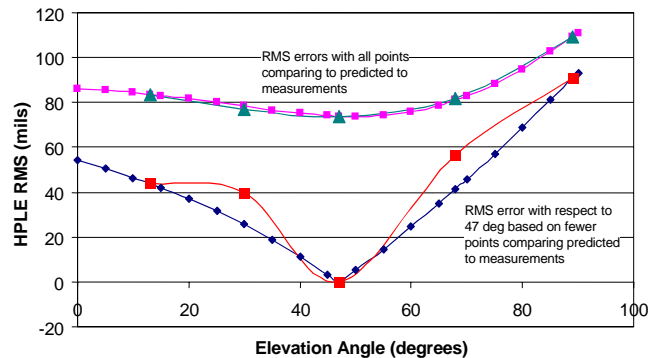


Figure 7 – Summary of Predicted vs Measured Surface RMS and Gravity Deformation for DSS-14

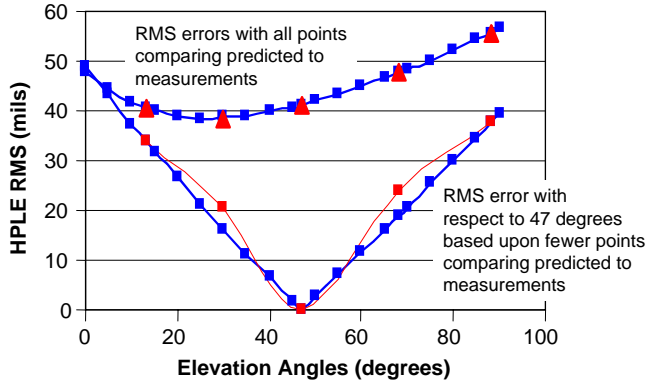


Figure 8 – Summary of Predicted vs Measured Surface RMS and Gravity Deformation for DSS-43

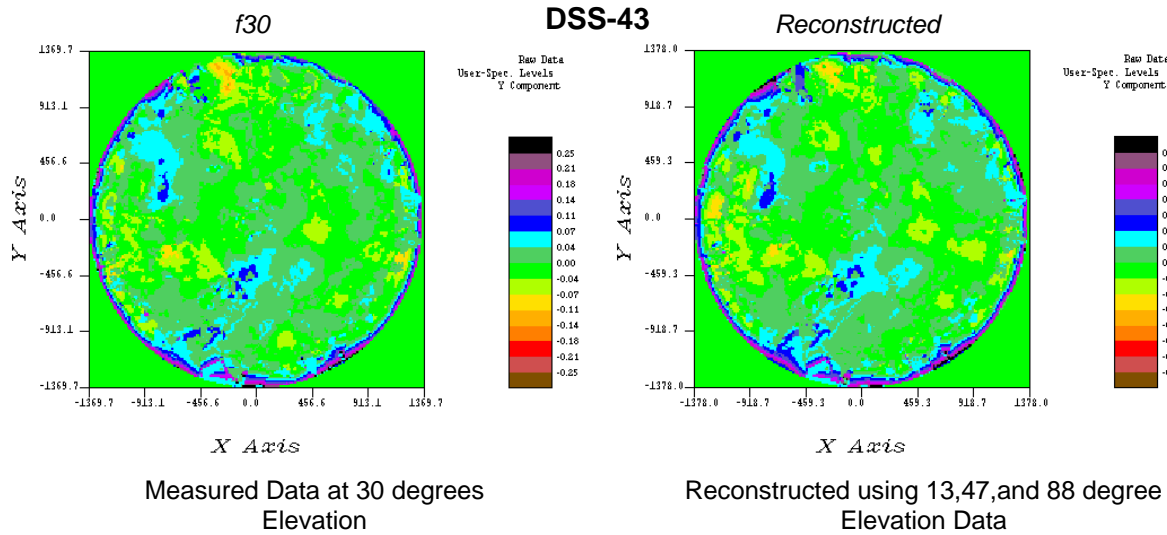


Figure 9 – Measured and Reconstructed Data at 30 degrees Elevation

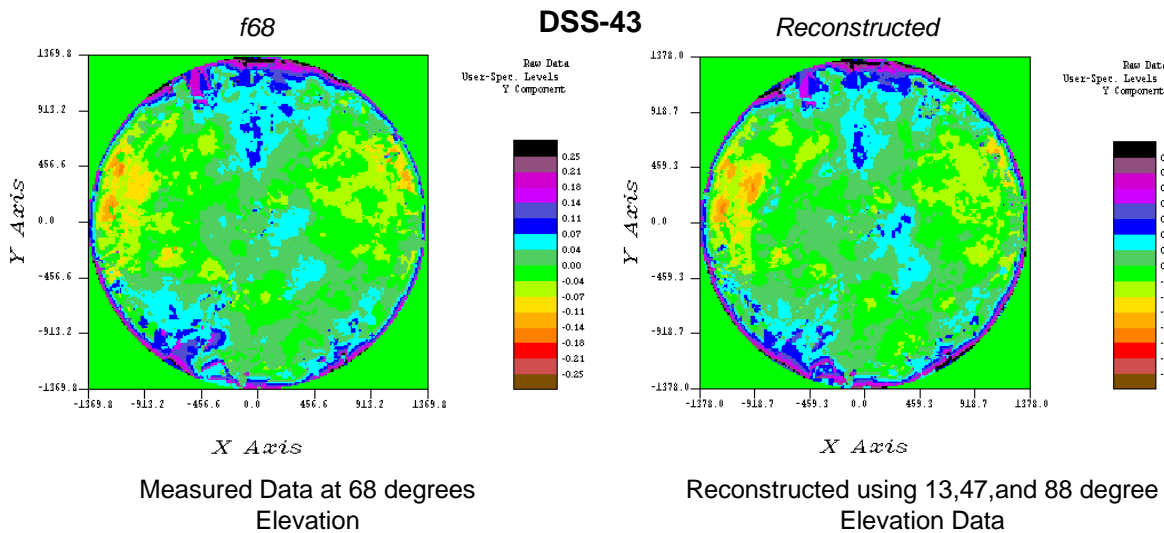


Figure 10 – Measured and Reconstructed Data at 68 degrees Elevation

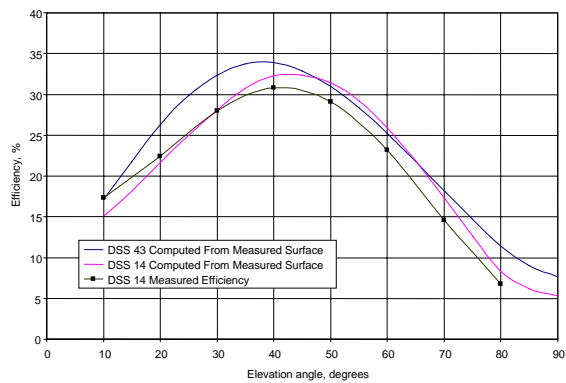


Figure 11 – Computed and Measured 70-meter Antenna Efficiencies